Optical Injection Locking of Ring Lasers in an Indium Phosphide Photonic Chip

*Damiano Massela Michael Wallace Ronald Broeke Francisco Diaz Nelson Pinto**

Damiano Massela, Dr. Francisco Diaz, Nelson Pinto
AtlanTTic research center, UVigo - Campus Universitario As Lagoas, Spain
nelson.filipe.duarte.pinto@uvigo.es
Dr. Michael Wallace, Dr. Ronald Broeke
Bright Photonics BV, Netherlands

Keywords: *Laser, Photonics, Semiconductor Photonics*

A large telecommunication bandwidth is fundamental for the networks of the future. Integrated photonics offers new solutions in terms of optical manipulation for these networks. Integrating lasers on a chip reduces cost, footprint, and energy usage. Nevertheless, direct laser modulation remains a constraint, causing reduced bandwidth. Optical Injection Locking (OIL) on integrated ring lasers promises to be a key technology for improving direct laser modulation and communications bandwidth. However, it is still lacking experimental validation.
In this study, two designs of optically injection-locked ring lasers were produced using monolithically integrated photonic circuits. The initial circuit characterization suggests these techniques are viable on integrated photonics platforms. These circuits pave the way for future applications in Quantum Key Distribution and coherent communication.

1 Introduction

The ever-increasing demands on telecommunication transmission bandwidth make the search for new technical solutions an extensive research topic. New techniques capable of increasing the transmitter bandwidth are emerging, notably those involving light modulation devices such as lasers. Optical Injection Locking (OIL) [1] is one of those techniques, which has the advantage of directly modulating a laser to a higher bandwidth than allowed by direct modulation. Studies show that it is possible to reach bandwidths of up to 100GHz [2].
The emergence of quantum computing technologies created a debate over current telecommunication security systems. Quantum computers have the potential to break some of the current encryption technologies used across our communication networks. More than just a technical problem, this issue could cause significant problems in our network-dependent society. Techniques such as Quantum Key Distribution (QKD) have been developed to overcome this problem. These techniques use photon properties to transmit encryption keys over networks securely [3].
Photonic Integrated Circuits (PICs) are a technology where optical components can be integrated into a chip, creating complex systems in a small package. The benefits of high component integration on a small footprint, with increased functionality at low energy consumption, make this technology a key technology for the next decades. Current transmission systems require a large number of optical components, allowing data transmission through dozens of channels on the same medium and effectively a large bandwidth. However, these components are sometimes bulky and limit the implementation scalability. To accommodate an even larger bandwidth and increase transmission efficiency, PICs are a particularly appealing technology which can overcome the scalability issue [4]. They offer a potential solution for combining a large number of optical components into a single chip, which is critical to increasing network throughput. At the same time, they are versatile and permit the usage of different applications such as QKD.
Extensive studies on OIL systems have been reported [5, 6, 7], but no experimental realisation has been shown to date. OIL consists of synchronising emission frequency and phase of two inter-connected lasers. The light of a primary master laser is injected into a secondary slave laser, designed to have similar free-running emission characteristics. If their emission frequencies are close enough, the secondary laser is forced to synchronise with the primary laser frequency and phase. Besides a close frequency, also the

injected power rate influences the operation stability of the system, so an analysis based on laser rate equations must be done to evaluate the lasing capability.
Besides synchronisation, this technique presents better modulation bandwidth and reduced relative intensity noise (RIN) and chirp [8, 9], compared to other direct modulation techniques. It also provides a solution to reduce laser linewidth, as demonstrated in [10].
In this paper, two integrated photonics laser transceivers were designed and fabricated, covering both traditional and quantum telecommunications applications. The designs presented here show the OIL technique implemented on a monolithically integrated ring laser system fabricated through an Indium Phosphide (InP) multi-project wafer (MPW) run. Using InP allows the integration of laser sources, gain sections and photodiodes on the same chip, which is not achievable with other materials such as silicon. The primary intended chip usage is QKD, with a design similar to the one in the work of Sibson et al. [11]. It uses a technique described by [12] that exploits the OIL technique to modulate signals without using any modulators. The first circuit consists of a Distributed Feedback (DFB) Laser, the primary laser, optically locking a secondary ring laser. A gain section on the ring laser modulates the light intensity. The second circuit is realised using two-ring laser circuits fed by a master Distributed Bragg Reflector (DBR) laser. Each slave laser can be directly modulated, changing the intensity of its emission. A phase shifter is added on one circuit to set the dephase between both circuit outputs to 90 degrees, which turns this circuit into a traditional coherent transmitter.

2 Circuit Design

This section will briefly describe the two designed circuits and their components.

2.1 Single ring laser circuit

Figure 1 presents the first circuit schematic. We used the light from a simple DFB laser (designated master laser) to inject a ring laser (slave laser) optically. The master laser is based on a standard DFB laser module from the InP foundry, designed to emit at $1550nm$, and with one of the outputs terminated with a photodiode. This photodiode, also from the default InP building blocks, will characterise the DFB laser's emitted power. The ring laser is created using two multimode interferometers (MMI) as couplers. The MMIs used are $2x2$ ports, connected as shown in Figure 1. The additional unused port on each MMI is terminated using a photodiode. These photodiodes will enable the measurement of power circulating in both clockwise (CW) and counterclockwise (CCW) directions inside the ring cavity. These MMIs are customised and designed to split power unequally, as 85% on the cross output and 15% on the bar output. We have chosen this ratio to reduce the losses inside the ring and have a shorter gain section.

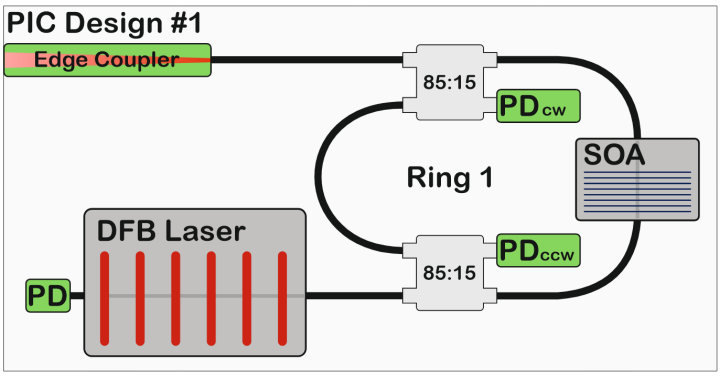

Figure 1: This schematic represents the layout of the first circuit design of OIL ring laser. The light of a DFB laser injects the ring laser.

The ring laser gain section uses a standard InP semiconductor optical amplifier (SOA) dimensioned to be $400\mu m$ long, which has been electrically connected using RF lines. This will allow us to drive and

modulate the ring laser. A spot-size converter is placed at the output of the circuit to minimise the losses when coupling the laser light output to an external fibre.

2.2 Double ring laser circuit

The second circuit is schematised in Figure 2, and the two rings are named *ring 1* and *ring 2*. In this case, we exploit the two outputs of a master DBR laser to OIL two slave ring lasers. The DBR master laser has three standard InP foundry components: DBR mirrors with a length of $30\mu m$, a $400\mu m$ SOA and a $200\mu m$ phase modulation section. These parameters ensure that the DBR laser has a high output power. The two outputs of the DBR laser are fed into two slave ring lasers that are identical in dimensions and components to the one from the first circuit. A phase modulator is connected to the output of one slave laser to obtain the $\pi/2$ phase shift required for coherent modulation. This additional phase modulation section comprises a thermo-optical phase modulator of length $450\mu m$, long enough to ensure the $\pi/2$ phase difference between the two outputs of the rings. The outputs of both slave rings are then combined into a single output by a $2x1$ MMI, followed by a spot size converter.

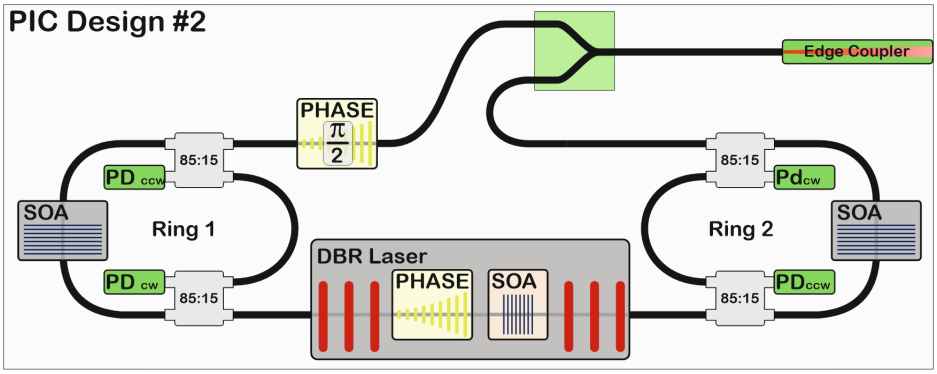

Figure 2: This schematic represents the layout of the second OIL ring laser design. Both outputs of a DBR laser are used to inject light into the ring lasers. The $\pi/2$ phase shifter can be seen in the output of ring 1.

The two circuits presented in this work were fitted to an InP MPW cell with dimensions $8mm\ x\ 2mm$, highlighting the small footprint of both circuits in comparison to traditional modulator-based circuits. The fabricated chip can be seen in Figure 3.

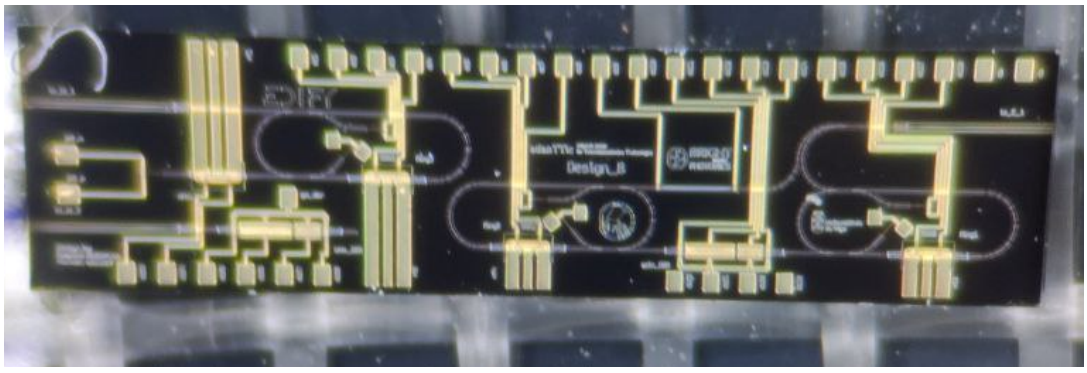

Figure 3: Photo of the manufactured photonic circuit under a microscope. The first circuit can be seen on the left side, while the second is on the right side of the chip. The metal pads for electrical connections can be seen on the top and bottom of the chip, while the optical connections are done on the left and right sides.

3 Simulated and Measurements results

The following sections will present the preliminary characterisation results of the circuit's basic functionalities.

3.1 Single ring laser circuit

The individual component's behaviour was verified before making a complete circuit characterisation. To test the DFB laser functionality, we used the coupled photodiode to measure the power response when feeding it with a variable current. When analysing the emission of the DFB laser, it became immediately evident that there had been some problems in the fabrication. The measured threshold current is relatively high compared to the value from the design manual, above $60mA$ against the expected $25mA$. Figure 4 shows the obtained Light-Current-Voltage (LIV) curve, representing the DFB laser optical output power depending on the injected current. A bell-shaped plot can be seen, where the heat and gain saturation effects decrease the power delivered after $95mA$.

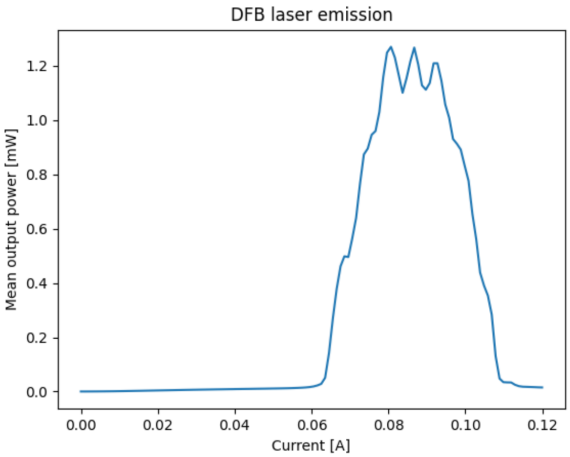

Figure 4: Measured LIV curve for DFB laser.

We have measured other DFB lasers fabricated in the same MPW run, and the threshold current ranges from $44mA$ to $60mA$ with maximum emitted power above $1mW$ only in one case. The fabrication report later confirmed the observed variability in the component behaviour. Aside from that issue, some measurements have been done, but considering that the master laser has a performance that deviates from the expected values. This imposes a limit on the injected light power, which can affect the locking stability.

To estimate the ring MMI performances, we drove the DFB at $80mA$, resulting in a current at the DFB photodiode of $-80\mu A$, whereas the MMI cross port photodiode registered $-60\mu A$. Both the photodiodes were biased at $-2V$ during the measurement. Assuming a $1dB$ loss for this kind of component, we reach the result that the splitting ratio of the MMI is 83% for the cross port and 17% for the through port. This ratio is close to the designed $85:15$, accounting for the fabrication variability.

To measure the real ring response, we coupled an optical power meter to the chip output and set the SOA feed current at $100mA$. Using the photodetectors of the chip, we measured the received power in both directions, obtaining the plot of Figure 5. The clockwise direction shows a weaker power than the counterclockwise direction, attributed to internal DFB circuit reflections. The measured power curve also diverges from the simulation linear result, presenting the same bell-shaped curve of the DBR laser.

The ring laser was simulated with the tool Phisim, obtaining a comb-like spectrum of Figure 6, when using a feed current of $100mA$. A limitation on Phisim simulating frequency-dependent effects causes the gain spectrum to be flat and an almost uniform spectrum. To test the real ring laser spectrum, we drove the ring 1 SOA at $100mA$ and coupled an optical spectrum analyser, obtaining the spectrum on the right side of Figure 6. We can notice that in this case, the output is a single mode with many small intensity peaks representing the cavity resonances and the frequency comb in the low power regime. The single emission peak is caused by cross-gain saturation and internal reflections from several components. However, the lasing spectrum is unstable and tends to jump, with side modes appearing and disappearing, following non-predictable fluctuations. This is due to the ring laser's inherent multi-mode nature.

To verify the optical locking of the system, we set a current of $97mA$ to the DFB master laser and $100mA$ to the ring 1 SOA. The obtained spectrum can be seen in Figure 7. When comparing both spectra of

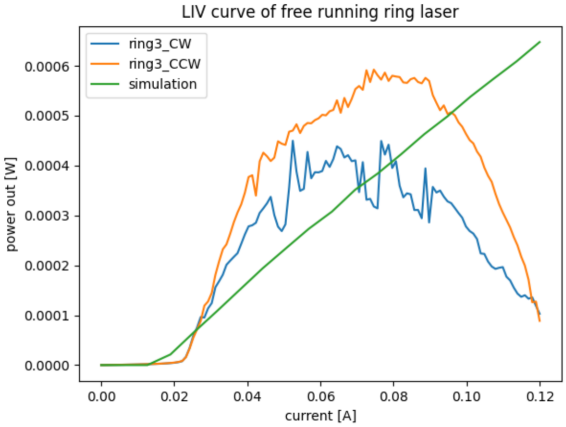

Figure 5: Measured LIV curve for ring 1 laser.

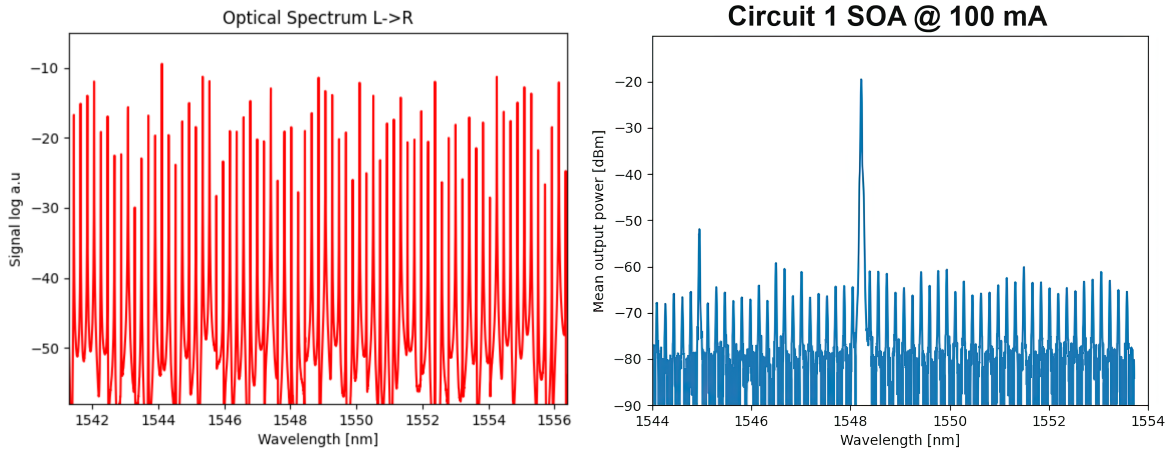

Figure 6: Simulated spectral response of the ring 1 laser (left side plot) and measured spectrum (right side), with the SOA driven at $100mA$.

single ring laser (Figure 6) and optically locked laser, we can see that the main peak is shifted from $1548.1nm$ to $1549.4nm$, while the secondary peak seen in Figure 6 at $1545nm$ disappears. This peak maintains stable in the same wavelength. This behaviour demonstrates that the system works as expected, with the DFB laser output locking the ring laser response.

The measured power at MMI photodiodes can be used to further verify that OIL is working. When locked, we measured the current at the MMI's photodiodes, mainly in the CCW direction.

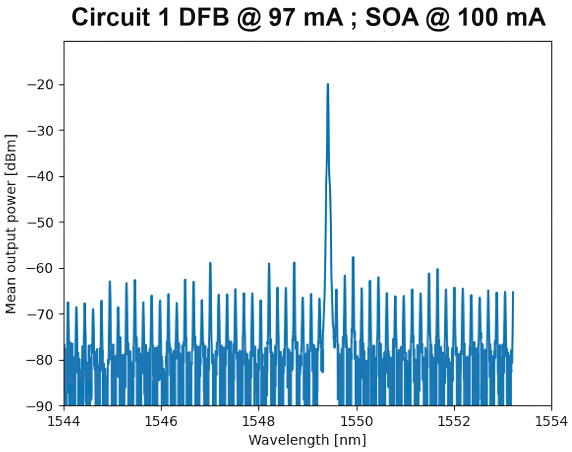

Figure 7: Measured spectral response of the optically locked ring laser, with DFB fed with $97mA$ and SOA driven at $100mA$.

Without DFB laser injection (laser turned off), the ring laser emission is bidirectional, with the measured current on the CW photodiode being $-0.160mA$. Feeding the DFB laser with $97mA$ (laser turned on), the current measured on the CW photodiode reduces to $-0.002mA$, demonstrating the high suppression of the CW light. The ring laser's optical injection locking ensures the light's unidirectionality inside the cavity, completely suppressing the CW mode.

3.2 Double ring laser circuit

To evaluate the second circuit, we independently characterised the DBR laser's LIV curve, as presented on the left side of Figure 8. The measured threshold and curve shape diverged from the simulated ones, but we do not have a valid reason for it. Simulation done on similar lasers gave accurate results, so we suspect that some variations in the manufacturing process can have an influence on this response.
The design of the DBR laser was focused on having a high power output, sacrificing the single-mode emission, which can be seen on the simulated spectrum of the right side Figure 8. We will use the OIL not only for isolating a single frequency of the slave lasers but also to isolate a single frequency of the DBR master laser.

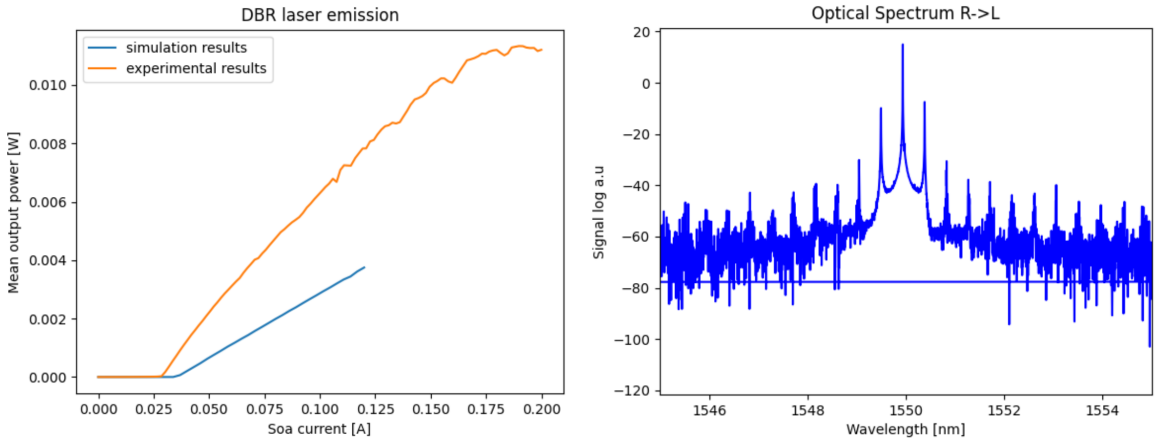

Figure 8: Measured LIV curve for DBR laser and simulated spectrum.

We characterised ring laser 1 individually, which has a similar construction to ring 1 from the first circuit. The main difference is the DBR mirror feedback from the master laser that changes the behaviour of the ring, giving it a preferred lasing direction. Analysing the ring 2 LIV response we obtained the curve of figure 9. Here, we can see a close agreement from the simulated threshold current but with a higher slope on the measured curve.

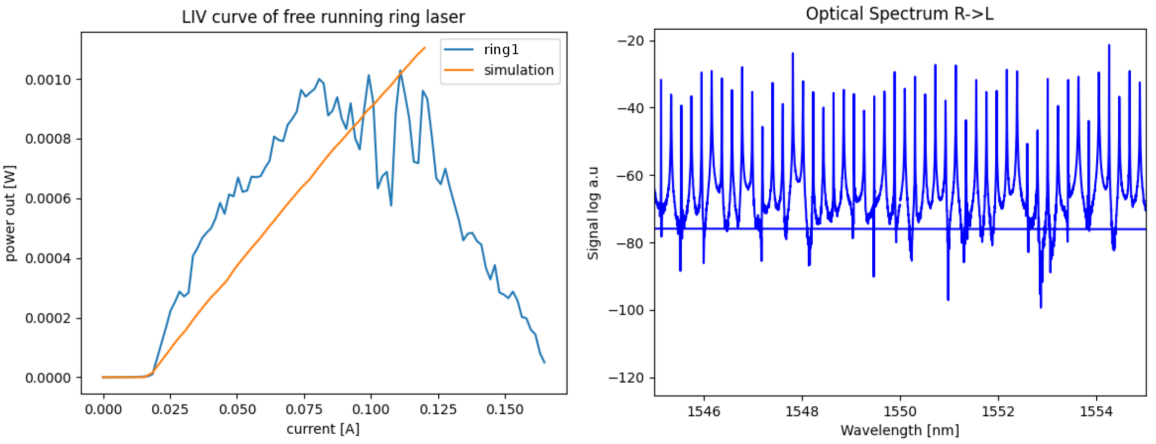

Figure 9: Measured LIV curve (left side plot) and simulated spectrum (right side plot) for ring laser 1.

This slope disagreement came from underestimating the gain coefficient used in laser simulations. The

simulated spectrum of this ring can be seen on the right plot of figure 9, with the comb shape visible. We fed the ring 1 SOA with a current of $60mA$ and obtained the left side spectrum of Figure 10, which, similarly to the ring 1 laser from the single ring circuit, shows an unstable single peak around $1553.3nm$. To verify optical locking, we first set and measured a single ring laser individually to test optical locking. The right side plot of Figure 10 shows the measured output of the ring 1 laser when injected with the light from the DBR laser. The laser emission is a stable single mode at $1550nm$, with a side-mode suppression ratio of $45dB$, demonstrating the locking of the two lasers. We do not see the multi-mode emission of the DBR laser nor any sign of the multi-mode of the ring laser. This shows that this system has effectively achieved OIL. The current applied to the SOA is critical and affects the locking mechanism, although we can find multiple combinations of currents that achieve OIL. In this case, we used a ring current of $55mA$ and a DBR current of $40mA$.

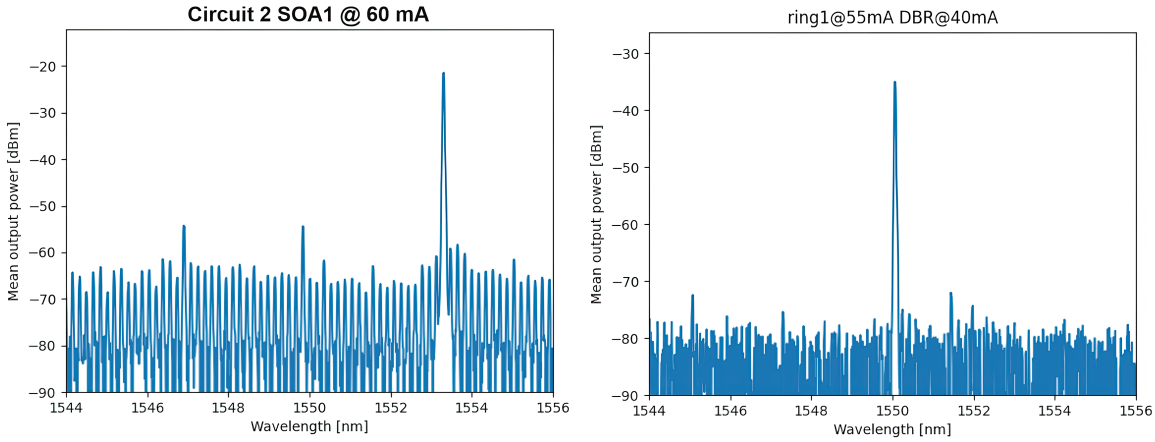

Figure 10: Measured spectrum for ring laser 1 (left side), and for ring laser 1 + DBR laser, locked emission (right side).

The next step was to verify if we could simultaneously lock both ring 1 and ring 2 to DBR laser mode. When the ring 2 laser is active, we notice that a series of other peaks appear in the spectrum in addition to the main peak from ring 1 (left side plot of figure 11). To achieve a stable locking of both ring lasers, we have varied the applied current fed to the different active components, but even the best outcomes have not been convincing. We have also decided to vary the phase modulator in the DBR laser to check its influence on the locking mechanism. We drove both SOA rings at the same constant current of $80mA$ and varied the currents applied to the DBR laser SOA and phase sections. The best-recorded spectrum is visible on the right side of figure 11, obtained with $77mA$ on the SOA and $29mA$ on the phase modulator of the DBR laser.

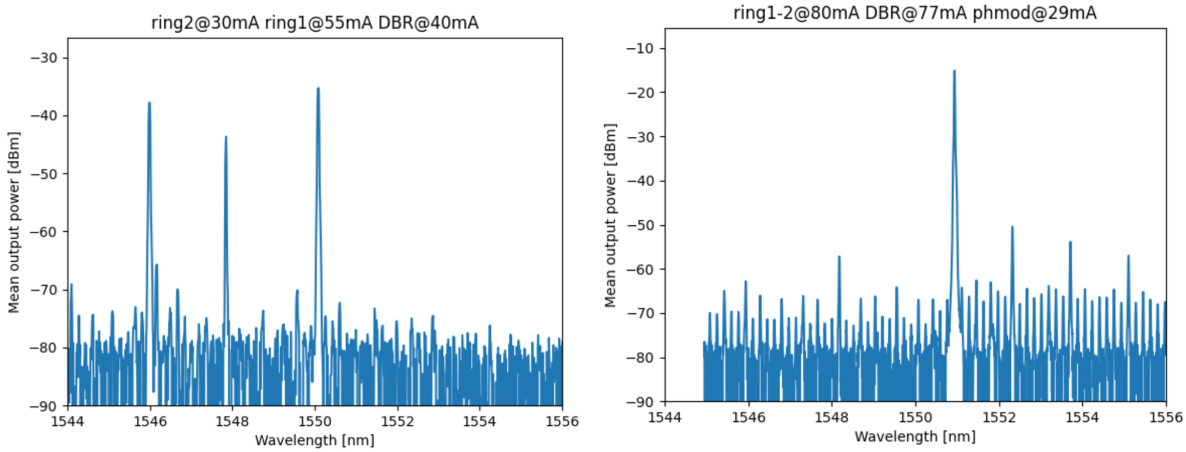

Figure 11: Measured spectrum both ring and BDR laser active (left side), and for DBR phase shifter tuned (right side).

From the resulting spectrum, we can see a main peak at $1551nm$ and a few side peaks roughly $35dB$ lower. It is clear that the system is not still locked, and the three lasers influence the emission of one an-

other, even if in an OIL system, they should be lasing in a single direction, as verified for the first circuit. In fact, if we turn ring 1 off the output spectrum goes back to being multimode.

4 Conclusion

This paper describes the designs and preliminary characterisation results on two OIL-based photonic integrated circuits, with potential applications on coherent communications and QKD.
The first circuit presented is based on a simple, easy-to-manufacture design that uses common and widely available components on several InP foundries. We have individually characterised the components, finding manufacturing problems with our master laser. The custom MMIs agreed closely with the designed specifications, achieving the expected splitting ratio. When considering the complete circuit, our characterisation results show that achieving OIL between the two lasers was possible, resulting in single-mode, single-direction emission. This is the first experimental verification of a monolithically integrated OIL system using ring lasers.
Based on a double-ring laser configuration, the second circuit also uses common InP components, making manufacturing easy. However, locking both rings simultaneously turned out to be a more complex task. We have characterised one of the ring lasers locked by the DBR laser, demonstrating that OIL can be achieved, performing as expected. When considering the locking of both ring lasers to the master DBR laser, we achieved only partial locking when using the DBR phase tuning section. These results are still not usable for coherent communications since, for this application, we need both lasers fixed to a single wavelength. Both rings must be locked for this design to achieve the desired high-speed modulation on QPSK modulation schemes.
In the future, we plan to investigate further the double-ring locking system, which presents some additional challenges to operate correctly. Moreover, we want to test and measure the modulation bandwidth of both circuits, as well as evaluate them in QKD applications. Due to the issue of broken manufactured lasers, these same designs must be redone in a new MPW run.

Acknowledgements
This research work was funded by H2020-MSCA-ITN-EID EDIFY N813467 and DRIVE-In N860763 grants.

References

[1] Liu, H., C. F. Lam and C. Johnson, "Scaling Optical Interconnects in Datacenter Networks Opportunities and Challenges for WDM," in *18th IEEE Symposium on High Performance Interconnects*, Mountain View, USA, August 2010, 113-116.

[2] Liu, Z. and R. Slavík, "Optical Injection Locking: From Principle to Applications," *Journal of Lightwave Technology*, Vol. 38, No. 1, 43–59, 2020.

[3] Qiu, J., "Quantum communications leap out of the lab," *Nature*, Vol. 508, No. 7497, 441–442, 2014.

[4] Tanaka, A., M. Fujiwara, K. Yoshino, S. Takahashi, Y. Nambu, A. Tomita, S. Miki, T. Yamashita, Z. Wang, M. Sasaki and A. Tajima, "High-Speed Quantum Key Distribution System for 1-Mbps Real-Time Key Generation," *IEEE Journal of Quantum Electronics*, vol. 48, No. 4, 542–550, 2012.

[5] Zhang B., R. Zhang, S. Xu, C. Luo and B. Qiu, "Modulation Response of Monolithically Integrated External Optical Injection-Locking Semiconductor Ring Laser Based on PPR Effect," *IEEE Photonics Journal*, Vol. 14, No. 2, 1–8, 2022.

[6] Duzgol, O., G. Kyritsis and N. Zakhleniuk, "Modulation dynamic response of optical-injection-locked wavelength-tunable semiconductor laser diodes," *IET Optoelectron.*, Vol. 11, 58–65, 2017.

[7] Chrostowski, L. and W. Shi, "Monolithic Injection-Locked High-Speed Semiconductor Ring Lasers," *Journal of Lightwave Technology*, Vol. 26, No. 19, 3355–3362, 2008.

[8] Sun, C., Liu, D., Xiong, B., Luo, Y., Wang, J., Hao, Z., Han, Y., Wang, L., and Li, H., "Modulation Characteristics Enhancement of Monolithically Integrated Laser Diodes Under Mutual Injection Locking". *IEEE Journal of Selected Topics in Quantum Electronics* , Vol. 21, No. 6, 628—635, 2015.

[9] Murakami, A., Kawashima, K., and Atsuki, K., "Cavity resonance shift and bandwidth enhancement in semiconductor lasers with strong light injection". *IEEE J. Quantum Electron* , Vol. 39, No. 10, 1196-–1204, 2003.

[10] Liu, Z., and Slavík, R., "Optical Injection Locking: From Principle to Applications". *Journal of Lightwave Technology* , Vol. 38, No. 1, 43-–59, 2020.

[11] Sibson, P., C. Erven, M. Godfrey, S. Miki, T. Yamashita, M. Fujiwara, M. Sasaki, H. Terai, M. G. Tanner, C. M. Natarajan, R. H. Hadfield, J. L. O'Brien and M. G. Thompson, "Chip-based quantum key distribution," *Nature Communications*, Vol. 8, 2041–1723, 2017.

[12] Yuan, Z. L., B. Fröhlich, M. Lucamarini, G. L. Roberts, J. F. Dynes and A. J. Shields, "Directly Phase-Modulated Light Source," *Physical Review X*, Vol. 6, 031044, 2016.

[13] Paraïso, T. K., I. De Marco, T. Roger, D. G. Marangon, J. F. Dynes, M. Lucamarini, Z. Yuan and A. J. Shields, "A modulator-free quantum key distribution transmitter chip", *npj Quantum Information*, Vol. 5, No. 1, 1–6, 2019.